Technical Paper https://doi.org/10.7733/jnfcwt.2021.19.2.243

A Study on Estimation of Radiation Exposure Dose During Dismantling of RCS Piping in Decommissioning Nuclear Power Plant

Taewoong Lee[1,*], Seongmin Jo[1], Sunkyu Park[1], Nakjeom Kim[1], Kichul Kim[2], Seongjun Park[2], and Changyeon Yoon[3]
[1]*Global Institute of Technology, KEPCO KPS, 211, Munhwa-ro, Naju-si, Jeollanam-do 58326, Republic of Korea*
[2]*Nuclear Maintenance Engineering Center, KEPCO KPS, Munsan 2Sandan-1ro, Oedong-eup, Gyungju-Si, Gyungsangbuk-do 38206, Republic of Korea*
[3]*Central Research Institute, Korea Hydro & Nuclear Power, 70, Yuseong-daero 1312beon-gil, Yuseong-gu, Daejeon 34101, Republic of Korea*

(Received March 29, 2021 / Revised April 14, 2021 / Approved June 8, 2021)

In the dismantling process of a reactor coolant system (RCS) piping, a radiation protection plan should be established to minimize the radiation exposure doses of dismantling workers. Hence, it is necessary to estimate the individual effective dose in the RCS piping dismantling process when decommissioning a nuclear power plant. In this study, the radiation exposure doses of the dismantling workers at different positions was estimated using the MicroShield dose assessment program based on the NUREG/CR-1595 report. The individual effective dose, which is the sum of the effective dose to each tissue considering the working time, was used to estimate the radiation exposure dose. The estimations of the simulation results for all RCS piping dismantling tasks satisfied the dose limits prescribed by the ICRP-60 report. In dismantling the RCS piping of the Kori-1 or Wolsong-1 units in South Korea, the estimation and reduction method for the radiation exposure dose, and the simulated results of this study can be used to implement the radiation safety for optimal dismantling by providing information on the radiation exposure doses of the dismantling workers.

Keywords: Individual effective dose, RCS piping, MicroShield program, NUREG/CR-1595, ICRP-60

*Corresponding Author.
Taewoong Lee, KEPCO KPS, E-mail: superdapo@kps.co.kr, Tel: +82-61-345-0554

ORCID

Taewoong Lee	http://orcid.org/0000-0002-7795-6188	Seongmin Jo	http://orcid.org/0000-0003-0754-5831
Sunkyu Park	http://orcid.org/0000-0002-8178-9415	Nakjeom Kim	http://orcid.org/0000-0003-3910-3616
Kichul Kim	http://orcid.org/0000-0001-5046-4127	Seongjun Park	http://orcid.org/0000-0002-9788-2294
Changyeon Yoon	http://orcid.org/0000-0001-8883-1404		

1. Introduction

Neutron activation or contamination by activation and corrosion products (Chalk River unidentified deposit: CRUD) cause high levels of activity in large components that are part of the primary circuit of a nuclear power plant (NPP) [1-3]. Hence, during the decommissioning of NPPs, the radiation exposure dose of dismantling workers should be estimated along with the establishment of a radiation protection plan to ensure radiation safety [4-6]. In previous research, the radiation exposure dose of dismantling workers was estimated using computer codes, with a focus on dismantling the main components because of the high radiation exposure dose. Thus, estimations of the radiation exposure dose during the dismantling of various contaminated components have been reported and analyzed [7-13].

Park *et al.* optimized the dismantling process for a research reactor and nuclear facility [7]. To estimate the radiation exposure dose of dismantling workers, a virtual dismantling environment was modeled, and the radiation exposure dose was calculated using the Monte Carlo N-particle radiation transport code version 4C (MCNP-4C) based on the inventory of radioactive materials. In 2010, Bonavigo *et al.* proposed cutting scenarios for main component segmentation by considering the radiological characterization of the primary system at the Enrico Fermi NPP in Italy [8]. Radioactive surface contamination of the primary circuit components and piping should be less than 1×10^4 Bq·cm^{-2}. In 2014, Jeong *et al.* analyzed the radiological characteristics to estimate the radiation exposure dose during the decommissioning of a reactor pressure vessel (RPV). The radioactivity of the RPV surface and concrete shield was calculated using the MCNP code [9]. The effective doses and their uncertainties during the dismantling of large-diameter pipes from the emergency core cooling system of the Ignalina NPP in Lithuania were evaluated in 2015 [10]. Four alternatives for dismantling the large-diameter pipes were considered. As a result, the optimal dismantling process, according to the cost analysis and the individual effective doses, was determined. In 2016, Hornáčk *et al.* presented dismantling scenarios for a steam generator and evaluated the radiological impact on the public and environment using external and internal radiation exposure doses [11]. In 2018, Lee presented an assessment of the radiation exposure dose resulting from decommissioning under the guidelines in Korea. The results were also compared and analyzed based on various overseas guidelines to evaluate the radiological environmental impact of NPPs [12]. To derive the optimal working time, the internal radiation exposure dose was compared and analyzed using various computer codes in 2018. The analyzed data, which were "as low as reasonably achievable" enabled the determination of the optimal working time [13].

In this study, the radiation exposure dose of dismantling workers at different positions was estimated using the MicroShield dose assessment program. The individual effective dose, i.e., the sum of the effective dose for each tissue considering the working time, was used to estimate the radiation exposure dose. The detailed dismantling process of a reactor coolant system (RCS) piping was analyzed based on the NUREG/CR-1595 report. The radioactivity due to the inner surface contamination of RCS piping was calculated by considering the decontamination factor (DF) and half-life of the ^{60}Co radionuclide. Finally, the individual effective dose in the dismantling process was estimated by considering the radiation exposure reduction methods.

2. Materials and methods

2.1 Detailed dismantling process of RCS piping

Based on the NUREG/CR-1595 report, the dismantling process of RCS piping is shown in Fig. 1 [14, 15]. Dismantling activities for chemical decontamination, cutting equipment installation, and nozzle and valve removal are often performed remotely. Most cutting operations are carried out using a bandsaw. Because dismantling workers perform both

Table 1. Tasks in the dismantling process [14, 15]

		Tasks	Types of Piping	Working time (man·h)	Distance (cm)
Preparation	a	Installation of scaffolding to permit access to all work areas	Hot-Leg	40	100
			Cold-Leg	40	
	b	Removal of insulation and installation of flame retardant	Hot-Leg	160	10
			Cold-Leg	160	
	c	Decontamination of exterior piping and installation of cutting equipment	Hot-Leg	81	
			Cold-Leg	81	
Removal	d	Cutting the pipe near the nozzle	Hot-Leg	112	10
	e	Cutting the pipe near the RCS isolation valve		112	100
	f	Cutting the pipe near the nozzle	Cold-Leg	112	10
	g	Cutting the pipe near the RCP		112	100

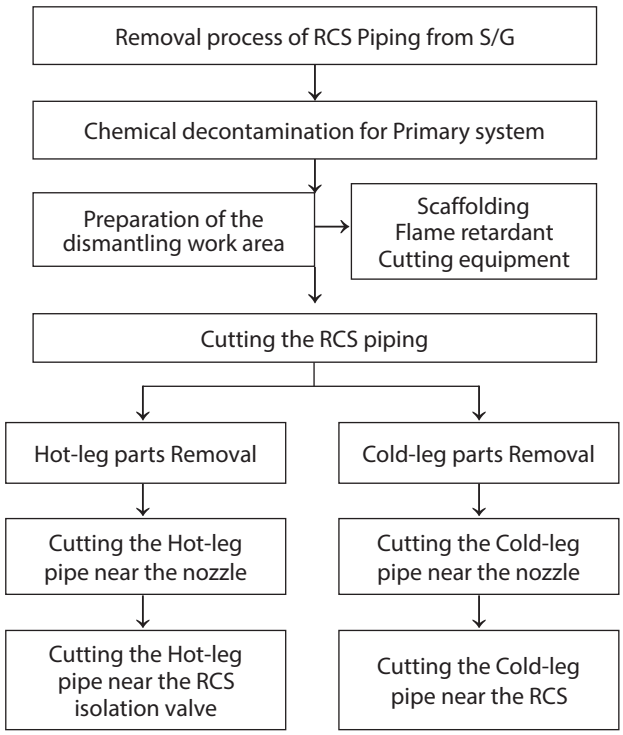

Fig. 1. Dismantling process of RCS piping in the decommissioning of a nuclear power plant [14, 15].

preparation and removal tasks, the distance between the radiation source and work areas varies depending on the requirements of the dismantling task. Table 1 summarizes the dismantling process of RCS piping, including the estimated working time and the distance between the radiation source and the work area.

2.2 Simulation input parameters of the MicroShield program

In the dismantling process, the radiological characteristics must be considered, such as the radioactivity of the inner surface contamination of components or the work area. In the primary coolant system of a NPP, the radioactive corrosion products (CRUD), which are activated by neutrons, results in an increase in the radiation exposure dose. Because the CRUD is saturated or deposited in the cold leg according to the concentration of hydrogen (pH), the radioactivity associated with the inner surface contamination of the cold leg is higher than that of the hot leg [16] (*cf.* Table 2). The most significant γ-ray-emitting radionuclides are ^{51}Cr, ^{54}Mn,

Table 2. Specifications and input parameters of RCS piping

Specification	Hot Leg	Cold Leg
Length of piping	200.0 cm	200.0 cm
External diameter of piping	128.3 cm	92.7 cm
Internal diameter of piping	106.7 cm	76.8 cm
Thickness of piping	10.8 cm	7.9 cm
Material of piping	Iron	Iron
Radioactivity of inner surface contamination for loop C ($Bq \cdot cm^{-2}$)	1.97×10^{2}	2.46×10^{3}
After decontamination (DF = 30, $Bq \cdot cm^{-2}$)	6.57	82

^{59}Fe, ^{58}Co, ^{60}Co, and ^{95}Zr [17]. When compared to other radionuclides, ^{60}Co radionuclide has a relatively long half-life and high energies (1,173 and 1,332 keV) and was therefore utilized to estimate the radiation exposure dose for dismantling workers. The radiological characterization data for RCS piping was obtained from actual measurements, which was then used for decommissioning at the Trino NPP in Italy [8]. The decommissioning of the Trino NPP, operated from 1965 to 1987, is planned to end by 2031. The primary system includes four primary loops from A to D, and each system consists of two valves and a reactor coolant pump (RCP). To conservatively estimate the radiation exposure dose, the maximum radioactivity of the inner surface contamination was selected from loop C of the primary system (Table 2).

The MicroShield program provides various geometric models for the evaluation of radiation shielding and estimation of the radiation exposure dose [18-20]. Moreover, the trends of the MicroShield results and the estimation of the Monte Carlo code were similar to each other in previous studies [21-22]. The total radiation dose ($Dose_{total}$) at the dose point was calculated using Eq. 1 based on the point-kernel method, which divides the volume source into a large number of small point sources, regards each as a point source, and obtains the sum of the respective contributions [18].

$$Dose_{total} = \int_E \int_V \left\{ \frac{C(E) S_0(E)}{4\pi V} \right\} \cdot B(E, \mu t) \frac{e^{-b}}{R^2} \, dV \, dE \quad (1)$$

where $C(E)$ is the flux-to-dose conversion factor ($Sv \cdot h^{-1}$ /#/$cm^2 \cdot s$) and $S_0(E)$ is the photon production rate (#/s). $B(E,\mu t)$ is the buildup factor and R is the distance from the source volume to the dose point (cm). b can be obtained as follows:

$$b = \sum_{i=1}^{N} \mu_i \, t_i \quad (2)$$

where μ_i and t_i are the linear attenuation coefficient of the i^{th} shield (cm^{-1}) and the thickness of the i^{th} shield (cm), respectively. The $Dose_{total}$ ($mSv \cdot h^{-1}$) at the dose point is integrated for the total photon energy and total source volume.

Table 2 lists the simulation input parameters, such as the geometry of the RCS piping and the radioactivity of the inner surface contamination [8, 14, 23]. In the MicroShield program, the calculated photon fluence rates at the dose points were converted into the effective dose. The weighting factors of radiation (W_R) and tissues (W_T) in the ICRP-60 report are the same as those in the ICRP-74 report [24, 25]. Because the weighting factors of the ICRP-60 dose model are used in Korea, the effective dose was calculated by applying the effective dose conversion factor of the ICRP-74 in the MicroShield program. The individual effective dose, which is defined as the sum of the effective dose to each tissue considering the working time, was used to estimate the radiation exposure dose. The detailed RCS piping dismantling

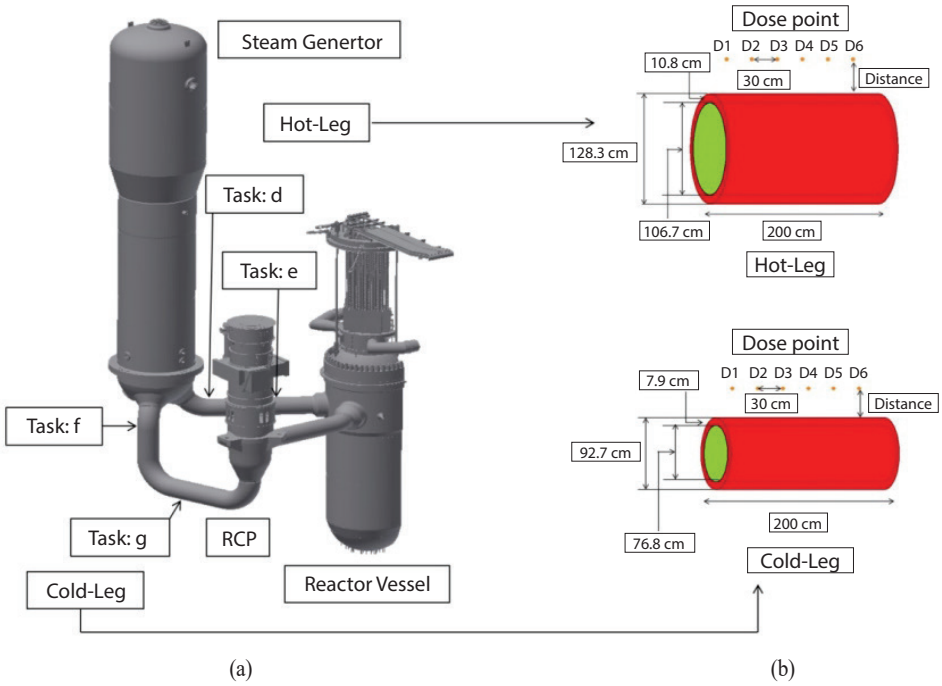

Fig. 2. Configuration of the RCS system: (a) RCS system and (b) schematic diagram of the simulation setup.

process was analyzed based on the NUREG/CR-1595 report. In actual dismantling tasks, the radiation exposure dose will be affected by not only the radiation source of RCS piping but also by various radiation sources, which were attributed to the various dismantling tasks. However, in this study, the radiation exposure dose for each dismantling task was estimated to provide information on the radiation exposure dose for the optimized RCS piping dismantling process design. The radioactivity of the inner surface contamination of RCS piping was calculated by considering the DF. The individual effective dose for the dismantling process was also estimated by considering the radiation exposure dose reduction methods, such as the decay with half-life of the ^{60}Co radionuclide and lead shielding.

The positions for the radiation exposure dose estimation and the simulation setup are illustrated in Fig. 2. Considering the structure of RCS piping, the geometry of the simulation was modeled by applying a cylinder surface-external dose point in the MicroShield program. The effective dose to each tissue and the individual effective dose were estimated and analyzed for the different positions of dismantling workers. Because the results of the radiation exposure dose estimation can be utilized for decommissioning the Kori-1 unit at the Kori NPP in South Korea, the DF was assumed to be 30, which is the target of DF for the unit [26]. Therefore, the radiation source terms using DF = 30 were used to estimate the radiation exposure dose in all dismantling tasks.

3. Results

3.1 Estimation of radiation exposure dose in dismantling tasks

After the detailed dismantling process for the RCS piping was chosen (Table 1), the radiation exposure dose of the workers dismantling the RCS piping was estimated by the

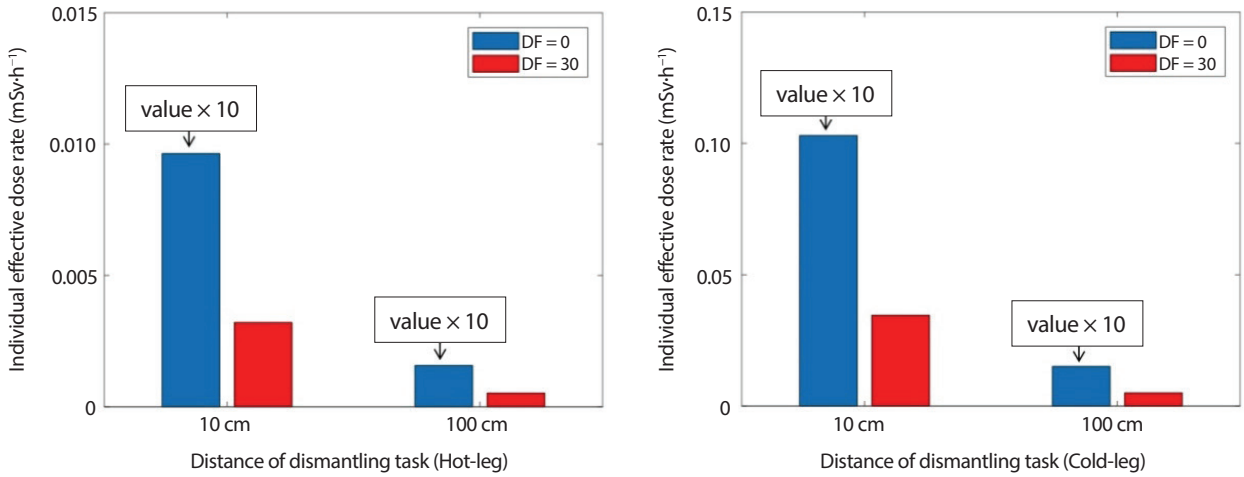

Fig. 3. Comparison of individual effective dose rates estimated by MicroShield program according to distance and DF values: (a) hot-leg and (b) cold-leg.

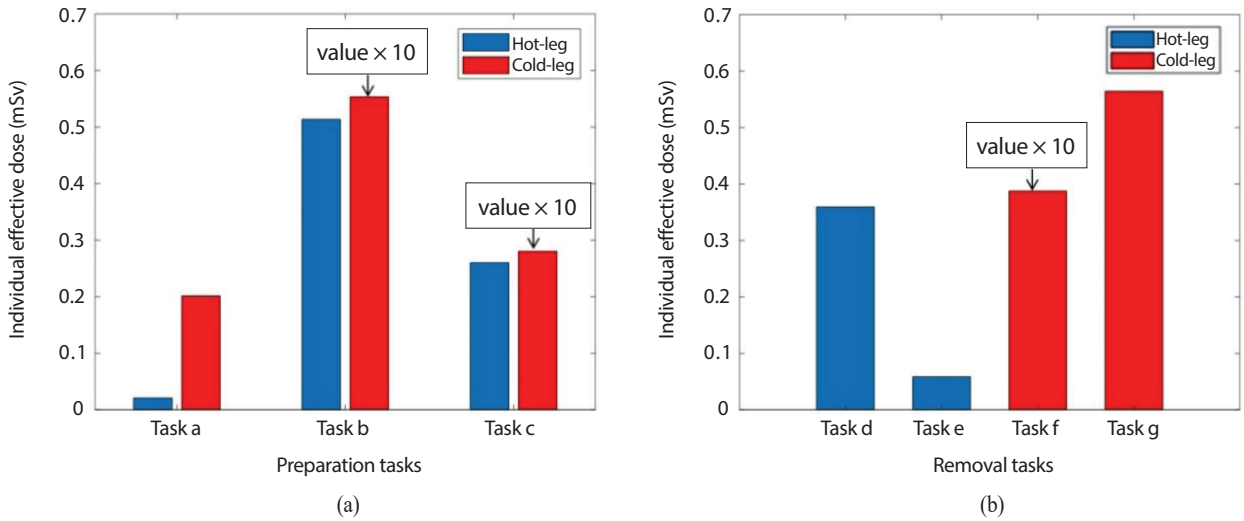

Fig. 4. Individual effective doses with DF = 30 for each dismantling task (Table 1): (a) preparation tasks and (b) removal tasks.

MicroShield program. The comparisons of the estimated individual effective dose rates according to the distance from the RCS piping are shown in Fig. 3. Because the radioactivity of the inner surface contamination of the cold leg was higher than that of the hot leg, the individual effective dose rates for dismantling tasks at the cold leg were higher than those at the hot leg. The individual effective dose rates decreased with increasing distance from the center of the RCS piping. As expected, the individual effective dose rates decreased by approximately one-third when radiation sources with DF = 30 were applied.

Fig. 4 shows the individual effective dose for each dismantling task. The individual effective dose of task B was the highest because it has the shortest distance from the radiation source and the longest working time. The individual effective doses of dismantling preparation tasks were higher than those of removal tasks because the latter were often performed remotely. Table 3 summarizes the individual

Table 3. Results of individual effective doses with DF = 30 for various dismantling tasks (Table 1)

		Tasks	Types of Piping	Individual effective dose (mSv)
Preparation	a	Installation of scaffolding to permit access to all work areas	Hot-Leg	2.09×10^{-2}
			Cold-Leg	2.07×10^{-1}
	b	Removal insulation and installation of flame retardant	Hot-Leg	5.14×10^{-1}
			Cold-Leg	5. 53
	c	Decontamination of exterior piping and installation of cutting equipment	Hot-Leg	2.60×10^{-1}
			Cold-Leg	2.80
Removal	d	Cutting the pipe near the nozzle	Hot-Leg	3.61×10^{-1}
	e	Cutting the pipe near the RCS isolation valve		5.85×10^{-2}
	f	Cutting the pipe near the nozzle	Cold-Leg	3.86
	g	Cutting the pipe near the RCP		5.64×10^{-1}

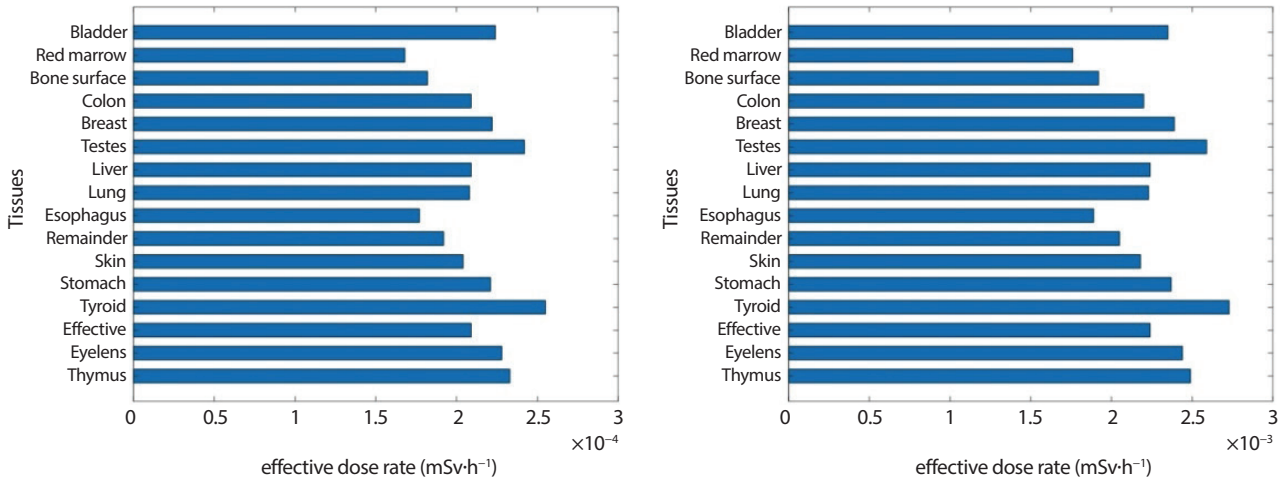

Fig. 5. Effective dose rates to each tissue in dismantling task B (DF = 30): (a) hot-leg and (b) cold-leg.

effective doses of dismantling tasks according to the defined distances between the radiation source and work area.

Fig. 5 shows the results of the highest effective dose rates to each tissue in dismantling task B. The effective dose rates to tissues with high radiosensitivity were high in all dismantling tasks. Based on the distance between the radiation source and the work area, the comparisons of the individual effective dose rates for dismantling tasks at various dose estimation points are shown in Figs. 6 and 7. The individual effective dose rates decreased with increasing distance between the center of the RCS piping and the estimated dose points. Therefore, to reduce the radiation exposure dose of dismantling workers, it is recommended that the cutting equipment be remotely controlled from the side of the RCS piping.

3.2 Comparisons of reduction methods for radiation exposure dose

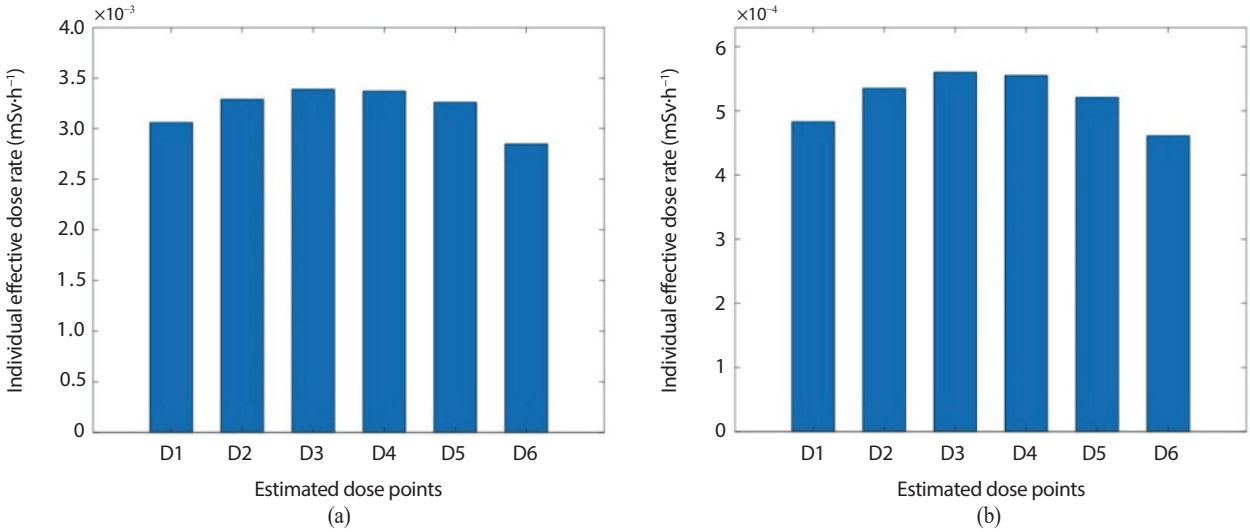

Fig. 6. Comparisons of individual effective dose rates of estimated dose points for dismantling tasks (hot-leg, DF = 30): (a) 10 cm and (b) 100 cm.

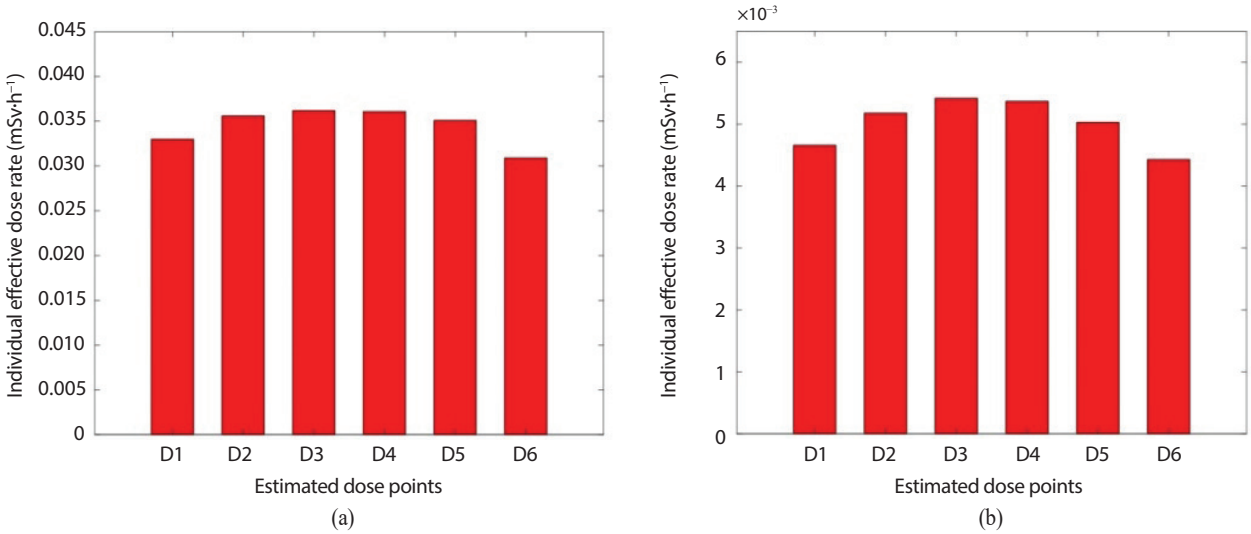

Fig. 7. Comparisons of individual effective dose rates of estimated dose points for dismantling tasks (cold-leg, DF = 30): (a) 10 cm and (b) 100 cm.

The radiation exposure dose of dismantling workers must remain stable. To reduce the radiation exposure dose of dismantling workers, we considered two radiation exposure dose reduction methods. First, the individual effective dose rates were calculated using the lead shielding typically used in NPPs. The thickness of the lead shielding was set to 3 mm [27]. As shown in Fig. 8, the individual effective dose rates with lead shielding are lower than those without lead shielding. The use of lead shielding resulted in dose reductions of approximately 15% to 30%.

Second, the decay of radioactive nuclides was used to reduce the radiation exposure dose. The major radioactive nuclide causing radiation exposure to dismantling workers is ^{60}Co, whose half-life is approximately 5.27 years. Thus, the dismantling of major components may begin approximately 10 years after permanent shutdown. Based on the results in Fig. 9 and Table 4, the individual effective dose rates for dismantling workers significantly decreased upon considering

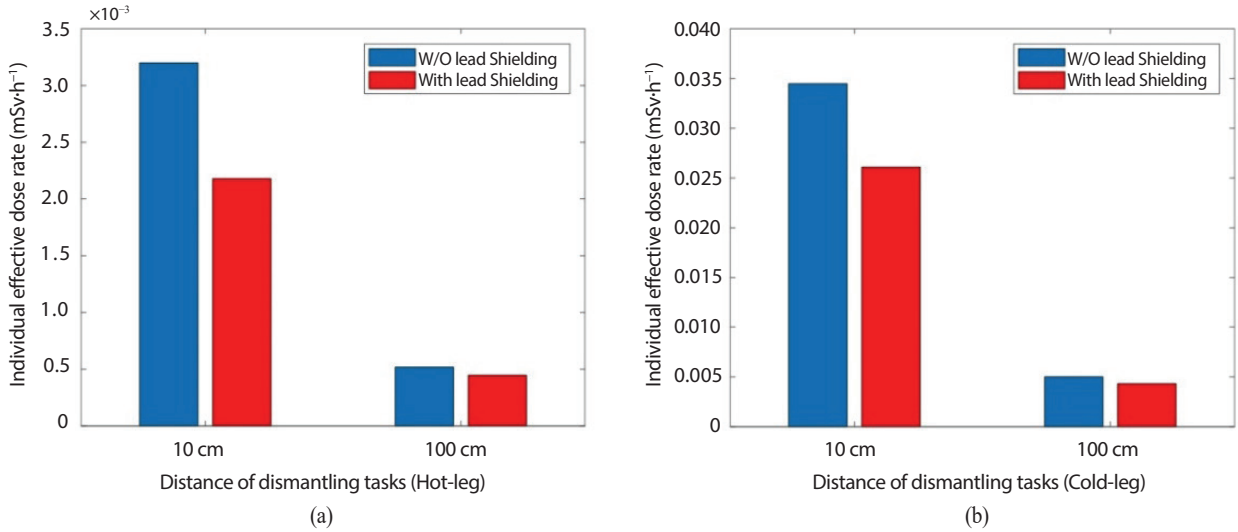

Fig. 8. Comparison of individual effective dose rates with and without lead shielding according to the distance of dismantling tasks: (a) hot-leg and (b) cold-leg.

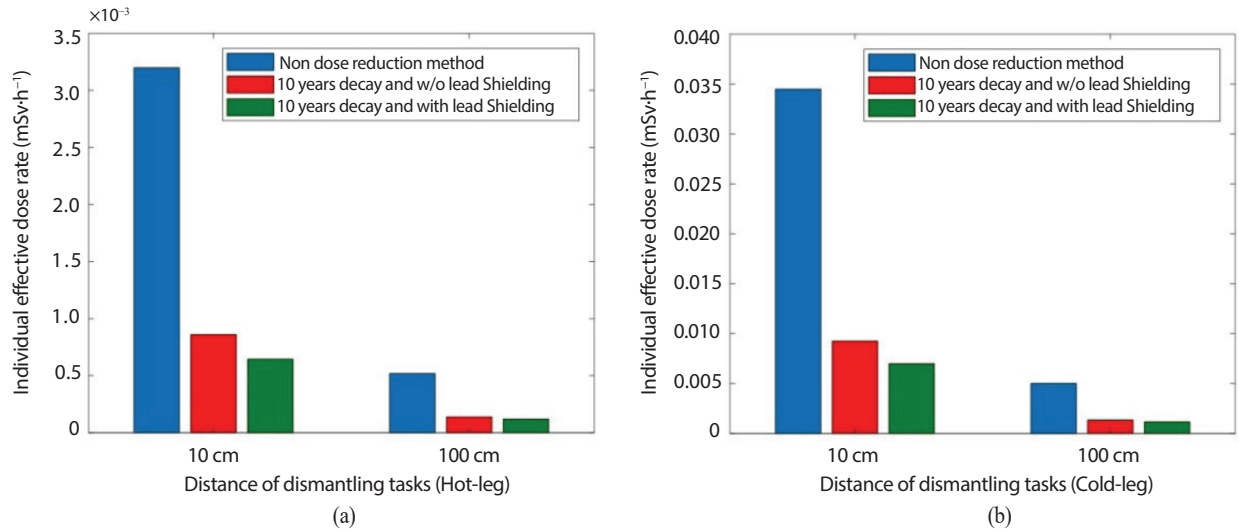

Fig. 9. Comparison of reduction method of radiation exposure dose for dismantling tasks (DF = 30): (a) hot-leg and (b) cold-leg.

the 10 years of decay and lead shielding. The effectiveness of the radiation exposure dose reduction using the radionuclide decay decreased by approximately 70% after 10 years.

4. Conclusions

Based on the characteristics of RCS piping dismantling tasks, the radiation exposure dose was estimated for dismantling workers at different positions using the MicroShield program. The individual effective dose, which is defined as the sum of the effective dose to each tissue considering the working time, was used to estimate the radiation exposure dose. The simulation results were compared in terms of the working distance, estimated working time, and methods for reducing the radiation exposure dose. Because the

Table 4. Individual effective dose rates using radiation exposure dose reduction methods

RCS piping	Distance	After radioactivity of inner surface contamination ($Bq \cdot cm^{-2}$), DF = 30		After 10 years, Individual effective dose rate ($mSv \cdot h^{-1}$)	
		1 year	10 years	Without lead shielding	With lead shielding
Hot-leg	10 cm	6.57	1.76	8.61×10^{-4}	6.45×10^{-4}
	100 cm			1.39×10^{-4}	1.20×10^{-4}
Cold-leg	10 cm	82	22	9.26×10^{-3}	7.00×10^{-3}
	100 cm			1.35×10^{-3}	1.16×10^{-3}

radioactivity of the inner surface contamination of the cold leg was higher than that of the hot leg, the individual effective dose rates for dismantling tasks at the cold leg were higher. However, the individual effective doses for preparation and removal tasks were below the dose limit of ICRP-60. The results of chemical decontamination, radioactive nuclide decay, and shielding planning demonstrate the reduction of the radiation exposure dose in the various RCS piping dismantling tasks. This study offers guidelines for the radiation safety of dismantling workers engaged in dismantling RCS piping.

REFERENCES

[1] International Atomic Energy Agency. Radiological Characterization of Shut Down Nuclear Reactors for Decommissioning Purposes, IAEA Report, Technical Reports Series No. 389 (1998).

[2] Electric Power Research Institute. Decommissioning Technology Experience Reports, EPRI Report, TR-10000884 (2000).

[3] R. Anigsein, H.J. Chmelynski, D.A. Loomis, S.F. Marschke, J.J. Mauro, R.H. Olsher, W.C. Thurber, and R.A. Meck. Radiological Assessments for Clearance of Materials From Nuclear Facilities-Main Report, U.S. Nuclear Regulatory Commission Report, NUREG/CR-1640 (2003).

[4] International Atomic Energy Agency. Decommissioning of Nuclear Power Plants and Research Reactors, IAEA Report, Standards Series No. WS-G-2.1 (1999).

[5] European Commission. Practical Use of the Concepts of Clearance and Exemption-Part 1, Guidance on General Clearance Levels for Practices, European Commission Report, Radiation Protection 122(2000).

[6] J. Kaulard and B. Brendeback, "Radiation Protection During Decommissioning of Nuclear Facilities-Experiences and Challenges", Proc. of the 13th International Congress of the International Radiation Protection Association, May 13-18, 2012, Glasgow.

[7] H.S. Park, S.K. Kim, K.W. Lee, C.H. Jung, and S.I. Jin, "Visualization of a Dismantling Environment for an Evaluation of a Worker's Dose During the Decommissioning of KRR-1&2", Ann. Nucl. Energy., 35(6), 1117-1124 (2008).

[8] L. Bonavigo, M.De. Slave, M. Zucchetti, and D. Annunziata, "Radioactivity Release and Dust Production During the Cutting of the Primary Circuit of a Nuclear Power Plant: The Case of E. Fermi NPP", Prog. Nucl. Energy., 52(4), 359-366 (2010).

[9] K.S. Jeong, B.S. Choi, J.K. Moon, D.J. Hyun, G.H. Kim, T.H. Kim, S.Y. Jeong, and J.J. Lee, "Radiological Assessment for Decommissioning of Major Component in Nuclear Power Plants", Ann. Nucl. Energy., 63, 571-574 (2014).

[10] A. Simonis, P. Poskas, G. Poskas, and D. Grigaliuniene, "Modeling of the Radiation Doses During Dismantling of RBMK-1500 Reactor Emergency Core

Cooling System Large Diameter Pipes", Ann. Nucl. Energy., 85, 159-165 (2015).

[11] M. Hornác ̌k and V. Nec ̌as, "Assessment of the Radiation Impact of Steam Generator Dismantling on the Workers, Public and Environment", Prog. Nucl. Energy., 91, 345-354 (2016).

[12] S.H. Lee, H.W. Seo, and C.L. Kim, "Preparation of Radiological Environmental Impact Assessment for the Decommissioning of Nuclear Power Plant in Korea", J. Nucl. Fuel Cycle Waste Technol., 16(1), 107-122 (2018).

[13] S.I. Kim, H.Y. Lee, and J.S. Song, "A study on Characteristics and Internal Exposure Evaluation of Radioactive Aerosols During Pipe Cutting in Decommissioning of Nuclear Power Plant", Nucl. Eng. Technol., 50(7), 1088-1098 (2018).

[14] G.R. Hoenes, M.A. Mueller, and W.D. McCormack. Radiological Assessment of Steam Generator Removal and Replacement: Update and Revision, Pacific Northwest Laboratory Report, NUREG/CR-1595 (1980).

[15] M.A. Parkhurst, L.A. Rathbun, and D.W. Murphy. Radiological Assessment of Steam Generator Repair and Replacement, Pacific Northwest Laboratory Report, NUREG/CR-3540 (1983).

[16] J.S. Song, T.B. Yoon, and S.H. Lee, "A Study on Corrosion Product Behavior Prediction for Domestic PWR Primary System by Using CRUDTRAN", J. Nucl. Fuel Cycle Waste Technol., 13(4), 253-262 (2015).

[17] N.M. Mirza, M. Rafique, S.M. Mirza, and M.J. Hyder, "Simulation of Corrosion Product Activity for Nonlinearly Rising Corrosion on Inner Surfaces of Primary Coolant Pipes of a Typical PWR Under Flow Rate Transients", Appl. Radiat. Isot., 62(5), 681-692 (2005).

[18] Grove Software. MicroShield User's Manual Version 10, Division of Grove Engineering, 2015.

[19] E. Michael, M. Dean J, and H. Lee. Dose Calculations From Source Models and Gamma-Ray Spectra, Sandia National Laboratories Report, SAND2020-2543 (2020).

[20] G.H. Chun, J.H. Park, and J.H. Cheong, "Calculation of Potential Radiation Doses Associated With Predisposal Management of Dismantled Steam Generators From Nuclear Power Plants", Sustainability, 12(12), 5149 (2020).

[21] A.D. Oliveira and C. Oliveira, "Comparison of Deterministic and Monte Carlo Methods in Shielding Design", Radiat. Prot. Dosimetry., 115(1-4), 254-257 (2005).

[22] I.M. Prokhorets, S.I. Prokhorets, M.A. Khazhmuradov, E.V. Rudychev, and D.V. Fedorchenko, "Point-Kernel Method for Radiation Fields Simulation", Probl. At. Sci. Technol., N5(48), 106-109 (2007).

[23] R.J. Belles, "Key Reactor System Components in Integral Pressurized Water Reactors (iPWRs)", in: Handbook of Small Modular Nuclear Reactors, D.T. Ingersoll and M.D. Carelli, 2nd ed., 103-122, Elsevier, Amsterdam (2015).

[24] International Commission on Radiological Protection, ICRP Publication 60: The 1990 Recommendations of the International Commission on Radiological Protection, Annals of the ICRP Publication 60 (1991).

[25] International Commission on Radiological Protection, ICRP Publication 74: Conversion Coefficients for Use in Radiological Protection Against External Radiation, Annals of the ICRP Publication 74 (1996).

[26] Y.J. Son, S.J. Park, J.H. Byon and S.Y. Ahn, "The Assessment and Reduction Plan of Radiation Exposure During Decommissioning of the Steam Generator in Kori Unit 1", J. Nucl. Fuel Cycle Waste Technol., 16(3), 377-387 (2018).

[27] J.I. Kim, B.I. Lee, and Y.K. Lim, "Analysis of a Lead Vest Dose Reduction Effect for the Radiation Field at Major Working Places During Refueling Outage of Korean PWR Nuclear Power Plants", J. Radiat. Prot. Res., 38(4), 237-241 (2013).